

The performances of undershot waterwheel with butterfly-shaped blades and the radius of grasshopper's elbow: The utilization efforts for river electrical energy potential

Suhartono^{1*}, Rahmad Rudianto², Sri Fatmawati³, Saiful Azis⁴

^{1, 2, 3, 4} Insitut Agama Islam Negeri Palangkaraya, Kalimantan Tengah, Indonesia

*Corresponding Address: suhartono@iain-palangkaraya.ac.id

Article Info	ABSTRACT
<p>Article history:</p> <p>Received: October 16, 2021 Accepted: March 12, 2022 Published: April 29, 2022</p> <hr/> <p>Keywords:</p> <p>Butterfly blade; Grasshopper elbow; Pico hydro; Undershot; Waterwheel.</p>	<p>Based on the amount of discharge or current, the river flows in Central Kalimantan have the potential to produce electrical energy. The purposes of this study were to design an undershot type of floating waterwheel and to test the effective bending angle at the radius of the grasshopper elbow in producing the most optimum power. This research uses experimental methods. The tools used are: mobile phone, multimeter, the gate of light, timer counter, flow rate, and the dimensions of the waterwheel diameter is 6 meters. Grasshopper angles vary from 0°, 30°, 45°, 60° and 90° with a submerged blade depth of 0.24 m. The results showed that the undershot waterwheel with a flexible pinwheel (like a grasshopper's elbow) produced a faster and more effective rotation than a wheel with a fixed pinwheel and blades. Because the waterwheel has a flexible pinwheel and the butterfly blades experience little resistance when moving in water, the wheel generates more electrical energy than a wheel with fixed pinwheels and blades. At the angle of bending of the radius of the grasshopper blade 30° with the butterfly blade, it produces more optimal electrical energy than angles 0°, 45°, 60°, and 90°. Suggestions for further research are to test the waterwheel in weak and medium current rivers.</p>
<p>© 2022 Physics Education Department, UIN Raden Intan Lampung, Indonesia.</p>	

INTRODUCTION

The utilization of renewable energy sources is the right alternative to overcome the limited access to electricity in Indonesia, especially in remote community areas (Warjito et al., 2018). The largest use of renewable energy sources and is projected to increase is electricity sources originating from hydropower Fields (Faria & Jaramillo, 2017; Kougiyas et al., 2019; Manzano-Agugliaro et al., 2017; Pérez-Sánchez et al., 2017; Punys et al., 2017; Punys et al., 2019).

One of the efforts to deal with a crisis in the field of electrical energy is to develop a type of small-scale hydroelectric power plant, pico hydro as an alternative way to utilize natural energy in the form of flowing water and as a way to protect the environment

and preserve it (Arias-Gaviria et al., 2017; Brykała & Podgórski, 2020; Krajačić et al., 2018; Nishi et al., 2015; Quaranta et al., 2017; Quaranta et al., 2020; Quaranta & Revelli, 2018; Quaranta & Wolter, 2021). Hydropower offers advantages over fossil fuels because it uses water as a renewable energy source and a sustainable energy supply (Ali & Kumar, 2017; Masud & Suwa, 2018; Zhou et al., 2019). Pico hydro is a type of hydroelectric power plant that produces electricity with an output power of less than 5 kW. Small-scale hydropower plants are receiving attention because of their high availability, suitable construction sites, and less impact on environmental damage (Balkhair & Rahman, 2017; McManamay et al., 2020; Nishi et al., 2020; Quaranta &

How to cite

Suhartono, S., Rudianto, R., Fatmawati, S., & Aziz, S. (2022). The performances of undershot waterwheel with butterfly-shaped blades and the radius of grasshopper's elbow: The utilization efforts for river electrical energy potential. *Jurnal ilmiah pendidikan fisika Al-Biruni*, 11(1), 1-17.

Revelli, 2017a; Sritram & Suntivarakorn, 2017; Moe et al., 2019).

The undershot wheel can operate at less than 2 m head so that it can be placed in small rivers in flat areas, close to population centers (Denny, 2004; Permanasari et al., 2019). The undershot waterwheel is recommended for electrification in remote areas in Indonesia because of its simple shape, which results in higher efficiency at low head conditions compared to other turbines (Warjito et al., 2018). The undershot waterwheel is recommended because of its effectiveness when operating at the low head (Moshfegh, 2011; Müller & Kauppert, 2004) in addition, because of its simple shape, the undershot waterwheel is an economical, efficient wheel, and many people know this technology (Quaranta & Müller, 2018) so that it is effectively applied in remote areas. The way the undershot waterwheel works is that if there is a flow of water that flows, it will hit the blade wall located at the bottom of the waterwheel (Setyawan et al., 2019).

The potential of water flow as Pico hydro scale electrical energy is found in rivers that flow throughout the year with maintained discharge, therefore it is important to realize the effective use of renewable energy sources, including high power hydroelectric energy at low cost. Waterwheels used as hydroelectric power can be broadly classified, namely waterwheels used in channels with high and low head/peak, and waterwheels used in open areas with very low head/peak channels (Irwan et al., 2019; Nishi et al., 2017; Nishi et al., 2020; Quaranta, 2018; Yahagi et al., 2016).

The Pico-hydro Power Plant requires heavy river flow to produce an optimum power (Fajri et al., 2019). Pico hydro has been widely used by developing countries such as Asian and African countries to generate electricity in remote areas due to lower life cycle costs, cheaper investment, and operating costs than solar photovoltaic (PV) and wind turbines (Adanta et al., 2020; Ho-Yan, 2012; Ming et al., 2018; Warjito et al., 2018). This is because Pico hydro-scale

waterwheels in the form of open channels can be applied on a small to medium scale in rivers and irrigation canals in various remote locations (Nishi et al., 2014; Nishi, et al., 2020).

Several locations in the world have great potential in the use of renewable hydro energy, such as the island of Kalimantan in Indonesia, it has hundreds of tributaries that flow throughout the year (Kholiq., 2015; Pranoto et al., 2018). The river topography pattern in Kalimantan has relatively flat characteristics with a low coastal shape and extends almost flat, the wider the shape of the river, the greater the volume of water going to the sea, there is also additional water from its tributaries, the water discharge varies according to the season so that the speed flow, water depth, and substrate composition vary according to flow length and river width which is influenced by tides (Lindawati, 2018; Norhadi et al., 2015). The undershot waterwheel is more suitable for river characters that have a low and very low head difference (Nishi et al., 2014; Nishi et al., 2020; Nishi et al., 2020).

The shape of the blades affects the level of performance of the wheel. Simulating the shape of a pinwheel with straight blades is more efficient than curved blades in a crossflow (Nishi et al., 2014; Nishi et al., 2020; Nishi et al., 2020). In addition, the performance of the mill is affected by the depth of the blade submerged in the water flow. Experimental analysis of the effect of the depth of the blade submerged by water flow on the undershot waterwheel shows the optimal value at a submerged depth of 40 mm compared to 20 mm, 60 mm, and 80 mm (Yah et al., 2016). The effectiveness of the number of blades and the shape of the blades for the undershot waterwheel shows that the highest performing model is the six blades in the shape of a tick (Jamlay et al., 2016), also previous research has provided many methods for improving the performance of the undershot wheel, such as modifications to blade geometry or concepts work, planning and design processes, use of appropriate

materials, and so on. Even though the development and application of this technology have taken decades, determining the appropriate number of blades is still based on assumptions (Jamlay et al., 2016; Warjito et al., 2018). Similar research that has been carried out, namely the performance of the undershot waterwheel with bowl-shaped blades shows that the bowl-shaped blade waterwheel is suitable as an alternative to small-scale power plants (Permanasari et al., 2019; Quaranta & Revelli, 2018; Sule et al., 2020).

This study aims to refine and improve the performance of the wheel in previous studies. This research varied the pico hydro scale undershot waterwheel with the geometric shape of the butterfly blade with the radius of the grasshopper's elbow. This is expected to improve the performance of the mill. This research also made improvements to the prototype from the original 2 meters diameter of the wheel to 3 meters and the number of pinwheels increased to 12 blades. Therefore, the purpose of this research is to design and manufacture a pico hydro scale undershot waterwheel with the geometric shape of a butterfly blade with the radius of the grasshopper's elbow, in addition to testing the performance of the wheel as shown by the electric power generated by the wheel.

This research intends to build an undershot waterwheel with a very low head and a waterwheel for open channels such as medium rivers and weak rivers. Wheel design with geometric shapes that can change flexibly, and it takes the form of animal limbs, namely butterfly wings, and grasshopper elbows. Previous research tested the type of butterfly blade waterwheel compared to a fixed blade turbine. The results showed that the butterfly blade was more efficient than the fixed blade (Suhartono et al., 2017). The results showed that the turbine output power and efficiency on a straight runner blade were greater than that of a curved blade (Nishi et al., 2015; Nishi et al., 2020). The pico hydro scale floating power plant engineering considers the condition of

the river's surface current which is not so heavy and drives the wheels as a rotating generator. Power plants are designed to rotate properly when on the surface of the water with weak currents, are affordable, and are easy to manufacture.

METHODS

The method used in this research is the experimental method. The data collection consists of measuring the speed of water flow, the generator rotational speed in rpm (rotation per minute), the amount of voltage, and the electric current on the lamp load. This measurement is based on the speed of the water pushing the blade of the wheel.

The output power (P_{out}) is then calculated using the following equation (Franco et al., 2019; Quaranta, 2018; Warjito et al., 2018):

$$P_{out} = \left(\rho \cdot g \cdot \left(\frac{d_1^2 - d_2^2}{2} \right) \cdot W \right) \cdot u \quad (1)$$

where the depth of the incoming water hits and pushes the blade (d_1), the depth of the water coming out of the blade (d_2), the width of the blade (W), the gravitational acceleration (g), and the density of the water (ρ), the speed of entry (u), with adds $d_2 = 0.5d_1$.

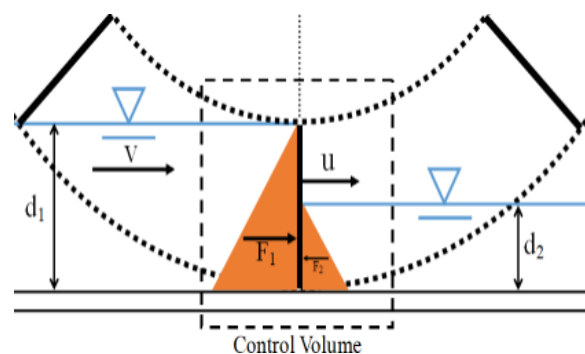


Figure 1. Hydrostatic pressure acting on vertical blades.

Collecting data in this study requires several instruments as shown in table 1.

Table 1. Data collection tools

	Tool	Quantity
1.	Mobile phone	1 piece
2.	Multimeter	2 pieces
3.	Gate of light	1 piece
4.	Timer counter	1 piece
5.	Flow rate (Pasco scientific)	1 piece

The following are the stages of data collection.

- a. The rate of water flow is measured using a flow rate. The measurement of water flow speed is done by placing the flow rate in line with the placement of the waterwheel (about 50 cm in front of the wheel) and the water flow. This is done so that the speed of the water flow regarding the flow rate is the same as the speed of the water that hits the waterwheel as shown in Figure 2.

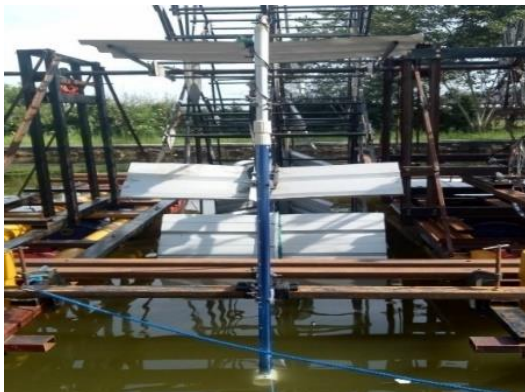


Figure 2. Installation of Flow Rate on the waterwheel

Figure 2 is a tool for measuring the speed of water currents. The tool is connected to a mobile phone via Bluetooth to see the values obtained through the SPARKvue application. The value that appears in the application is the value of the water flow velocity during the test.

- b. Measure the rotation of the wheel using the timer counter on the shaft of the wheel then see the time printed on the timer counter screen.
- c. Voltage and electric current are measured using a multimeter.
- d. The generator in this study functions as an energy converter in the waterwheel, which aims to get an overview of the function

and how much the waterwheel's performance is in producing electric power against changes in the speed of the water that drives the blade.

Instrument equipment for data collection in the pool can be seen in Figure 3.

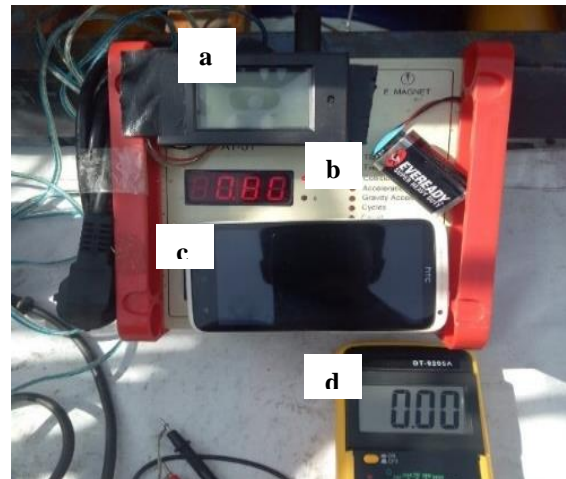


Figure 3. Instruments used in data collection Multimeter; b. Timer counter; c. Mobile Phone; d. Multimeter; e. Generator.

Figure 3 is the instrument used in data collection from the generator, namely 2 (two) multimeters, a timer counter, and a mobile phone. The multimeter is here used to measure the voltage and current generated by the generator when the generator is rotating. The timer counter is used to measure the rotational speed of the generator pulley. Mobile phone to see the speed of water flow as measured by flow rate. The data of measurement results are water velocity, generator rotation speed, and generator power. Permanent magnet generator (PMG) power capacity is 500 watts, 12-volt ac voltage, 3 phases, and a rotation speed of 600

rpm. The AC voltage generated by the PMG is then converted into a DC voltage, and rectified using an AC to DC rectifier. The voltage generated by the generator is stored in the accumulator (battery). This generator was chosen based on several considerations include being able to operate at low speeds, maintenance needs, and easy spare parts procurement.

The design and manufacture of the pinwheel were carried out in the physics laboratory of the Palangkaraya State Islamic Institute and data collection was carried out in the pool in the front yard of the IAIN Palangkaraya student dormitory which has a length of 20 meters and a width of 20 meters. The time of designing, manufacturing, and assembling the pinwheel for 5 months (March to July 2019) and the time of data collection in August 2019.

The speed of the water is obtained by pulling the wheel of several people. Figure 4 shows the flow chart of this research.

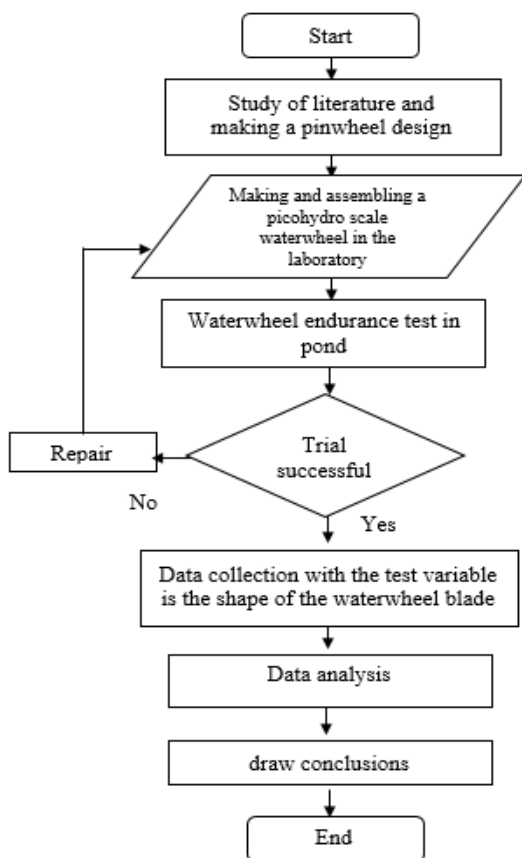


Figure 4. Research flowchart

RESULTS AND DISCUSSION

The design of the undershot-type waterwheel with the shape of a butterfly blade and the radius of the grasshopper's elbow that has been successfully made is shown in Figure 5. The wheel consists of 2 pieces which are attached to a buoy made of 6 PVC pipes and each is assembled with 2 pieces of PVC. The wheel buoys are also added with 12 empty drums which aim to strengthen the wheel buoy system. The wheel that is made has 12 blades with pinwheel spokes that are placed on an iron plate. The disc diameter is 60 cm. The floating pico hydro generating system consists of two waterwheels, a generator, a battery, and a buoy. The float is used to make the wheel hold the water. The dimensions of this waterwheel as shown in Table 2.

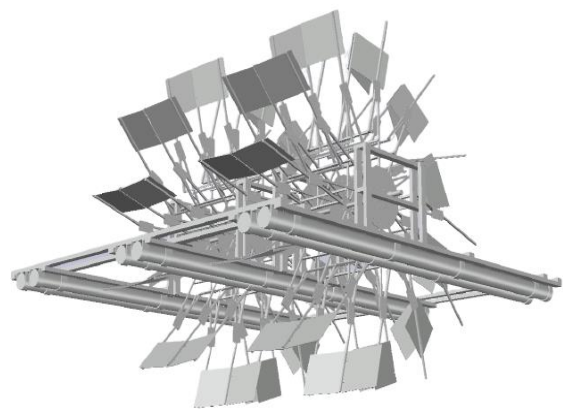
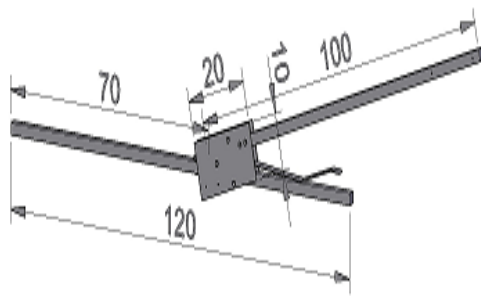


Figure 5. The undershot waterwheel that has been made and its dimensions

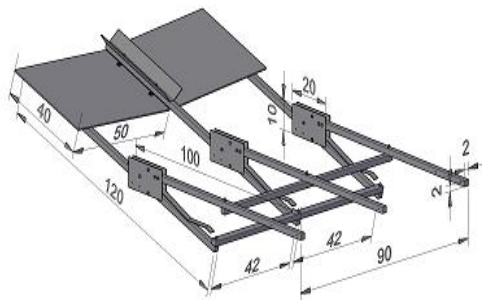
Table 2. Dimensions of waterwheel

	Waterwheel Component	Size
1.	Radius of Waterwheel	1.5 meters
2.	Construction width	5 meters
3.	Construction length	6 meters
4.	Shaft iron length	6 meters
5.	Number of blades per turbine	12 pieces
6.	Outer Diameter	3 meters
7.	Inner Diameter	2 meters
8.	Blade Length	1 meter
9.	Blade Width	0.4 meter

Figure 6 shows the dimensions of the radius in the shape of a grasshopper's elbow and the blade of a pinwheel in the shape of a butterfly's wings.



(a) The radius of the grasshopper's elbow



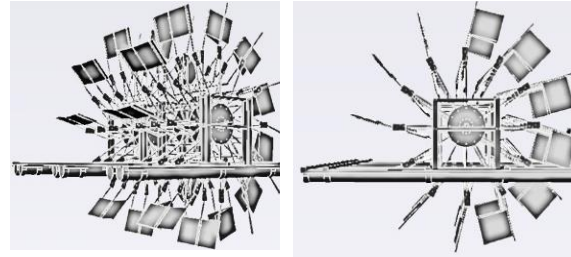
(b) The blade of the waterwheel is shaped like a butterfly wing

Figure 6. Waterwheels that have been made and their dimensions

Portable floating pico hydro is an efficient device compared to conventional devices (Dewatama et al., 2020). This system is relatively inexpensive and easy to operate and does not disturb the ecology of the river. The output power increases exponentially with the flow of water. The design of the floating power plant is made portable so that it is easy to use in areas where it is needed, cheap, and easy to maintain. All variables were measured with the same stages and treatments for each variation of fixed blades and butterfly blades.

In the butterfly blade wheel, the two parts of the blade can close and open by 90° . Changes in the rotation of the wheel when in the air after getting out of the water, the blade is closed and when it will enter the water the blade opens. The radius of the grasshopper's elbow also changes the distance from the center point of the wheel depending on the angle variation at the elbow, so that this

section experiences a flexible motion when the blade enters and leaves the water as shown in Figure 7.



a. The wheel is seen from an oblique position on the side. b. The wheel is seen from the side with the direction of the current and its rotation.

Figure 7. The Undershot Waterwheel with a Butterfly Blade and Grasshopper Elbow Radius

To adjust the bending angle of the grasshopper's elbow, use a restraint system (small bolt) at the point of bending the grasshopper's elbow so that the bending angle can be adjusted as shown in Figure 8

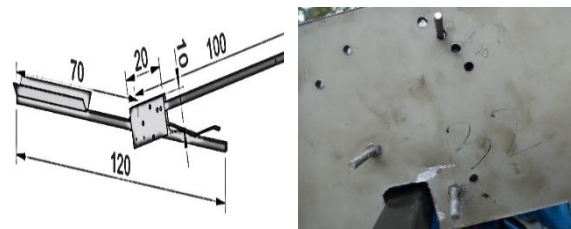


Figure 8. Adjusting the angle of the grasshopper's elbow bending.

The floating waterwheel test is carried out in a pond with a length of about 20 meters and a width of about 15 meters as shown in Figure 9, in the form of testing the water speed, generator rotational speed, voltage, and current generated by the generator at the effective depth of the submerged blade that has been determined from previous research, namely 0.24 meter from the depth. The whole blade is 0.44 meters, and the bending angle of the grasshopper's elbow is different from the variations. Data was collected by pulling a floating waterwheel from one end of the pond to the other, which is 15 meters away.



Figure 9. Wheel testing pool

The waterwheel output power is obtained by equation (1). Because this study uses 2 waterwheels, so the total power is 2 times the power of the wheel, as shown in table 3.

Table 3. Results of output power (P_{out}) and total power

v (ms^{-1})	u (ms^{-1})	P_{out} (watt)	$P_{total} = 2 \times P_{out}$ (watt)
0.40	0.20	42.57	85.15

v (ms^{-1})	u (ms^{-1})	P_{out} (watt)	$P_{total} = 2 \times P_{out}$ (watt)
0.50	0.25	53.22	106.43
0.60	0.30	63.86	127.72
0.70	0.35	74.50	149.01
0.80	0.40	85.15	170.29
0.90	0.45	95.79	191.58
1.00	0.50	106.43	212.87
1.10	0.55	117.08	234.16
1.20	0.60	127.72	255.44
1.30	0.65	138.36	276.73
1.40	0.70	149.01	298.02
1.50	0.75	159.65	319.30

$d_1 = 0.24$ m, $d_2 = 0.12$ m, $\rho = 1005.615$ kgm^{-3} ; $g = 9.8$ ms^{-2} ;

Table 4 shows the experimental test results of the butterfly blade waterwheel with several bending angles of the grasshopper's elbow. The variations in the bending angle are angel 0° , 30° , 60° , and 90° . The experimental results consist of generator speed and generator power at variations in water speed.

Table 4. The experimental results of the butterfly blade wheel experiment with variations of the grasshopper's elbow bending

water speed (m/s)	Angle 0°		Angle 30°		Angle 45°		Angle 60°		Angle 90°	
	Generat or speed (rpm)	Power (watt)	Generator rotation (rpm)	Power (watt)	Generat or speed (rpm)	Power (watt)	Generat or rotation (rpm)	Power (watt)	Generator rotation (rpm)	Power (watt)
0,4	83,23	6,70	105,17	10,08	142,54	11,43	161,32	18,39	200,86	34,39
0,5	90,28	7,88	108,01	11,49	121,36	10,60	169,05	20,09	155,40	23,80
0,6	100,12	23,26	140,99	17,49	195,76	11,32	183,37	25,20	224,43	53,70
0,7	106,18	27,72	164,90	24,38	186,80	36,96	198,23	31,22	234,01	57,62
0,8	115,65	24,51	177,33	28,57	203,25	31,95	209,82	37,13	231,00	50,48
0,9	120,26	31,17	214,65	40,53	209,34	38,44	222,83	44,44	276,37	71,07
1,0	170,54	46,28	212,09	45,00	229,45	51,41	232,65	57,24	280,64	62,57
1,1	205,21	58,71	224,57	71,62	235,70	57,68	252,53	65,67	272,36	62,79
1,2	216,91	65,66	264,67	87,22	244,50	65,18	264,17	77,80	251,99	67,35
1,3	230,33	73,52	259,06	79,47	253,21	79,21	291,00	106,88	230,86	59,70
1,4	240,65	85,94	279,04	106,63	270,20	94,34	283,96	115,60	273,47	102,75
1,5	280,45	121,45	304,52	157,66	291,12	105,71	293,36	120,51	276,27	104,54

Figures 10a and 10b present a comparison of the performance of waterwheels based on experimental values with variations in the bending angle of grasshoppers. The performance of the waterwheel is shown by the results of the

electric power and the rotation of the generator on the speed of the water. The speed of this water drives 2 rotating waterwheels that are connected to the pulley system to a generator that is given a lamp load of 200 watts. Two waterwheels are

attached on one axis. Electric power and generator rotation increase with increasing water speed. The theoretical analysis output power is calculated to be greater than the electric power converted by the generator rotation. The results of experimental calculations using a 200-watt lamp load

throughout the range of the speed of the water that drives the blade of the wheel.

The correlation between electric power and the rotation of the generator (RPM) to the speed of the water can be seen in Figures 10a and 10b.

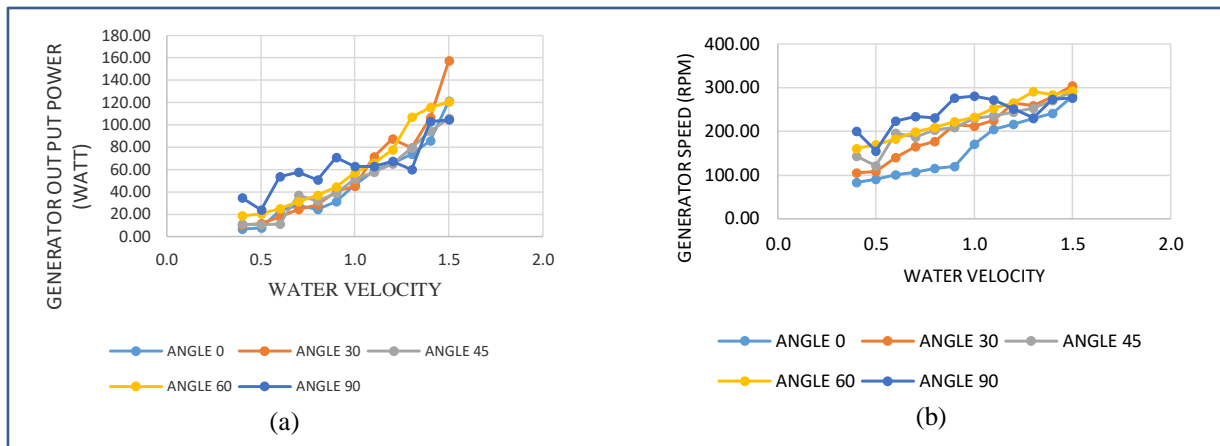


Figure 10. (a). Correlation of electric power to water speed. (b). Correlation of generator RPM rotation to the water speed

The output electric power of the generator has a characteristic value and shape. The output electric power will increase with the change in the speed of the water that drives the butterfly blade at every change in the bending angle of the grasshopper's elbow from 0° , 30° , 45° , 60° , and 90° as shown in figure 11.

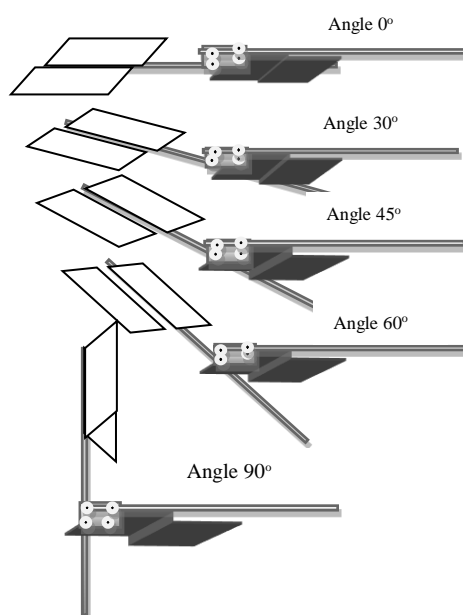


Figure 11. Bending angle of the grasshopper's elbows

Water velocity is the most important factor for undershot waterwheels (Denny, 2004). The shape of the constant radius of the bending angle of 0° is a reference for comparison to the range of electrical power at the load and the RPM generator rotation speed. This is seen in experimental values. The number of kinetic turbine blades is one of the variables that greatly affect the rotation and tangential forces that determine the power and efficiency of a kinetic turbine (Quaranta & Revelli, 2017b; Suparman, 2017).

Simultaneous measurement of electrical power with a 200-watt lamp load, generator rotation speed in rpm, and water speed. The measurement result shows the difference between the experimental value and the calculated result. The difference between experiment and analysis occurs mainly due to mechanical friction losses which are not considered in the calculations. The calculated efficiency of the waterwheel (η) is greater than the experimental value, except in the higher rotation speed range, the value is close to the experimental value. This can be seen

from the chart pattern. The results of the comparison of the experimental values of butterfly blade waterwheels with variations in the radius of the grasshopper's elbow show that the maximum output power and maximum efficiency of the wheel at a bending angle of 30° are around 49.38% at a water velocity of 1.5 m/s. The findings in this study have shown to some extent the qualitative characteristics of the performance of the butterfly blade undershot type waterwheel with variations in the grasshopper angle and flow plane of the waterwheel equipped with blades from different bending angles. The low efficiency of the wheel is probably due to the very low rotational speed (Quaranta & Müller, 2018). The design of the physical model of the waterwheel as a power plant where the results of this study show the relationship of flow velocity (cm/s) to energy (watt-hour) (Junaidi & Hendri, 2014).

The graph of the correlation between the generator electric power and water speed for the bending angle 0° on the pinwheels can be seen in Figure 12.

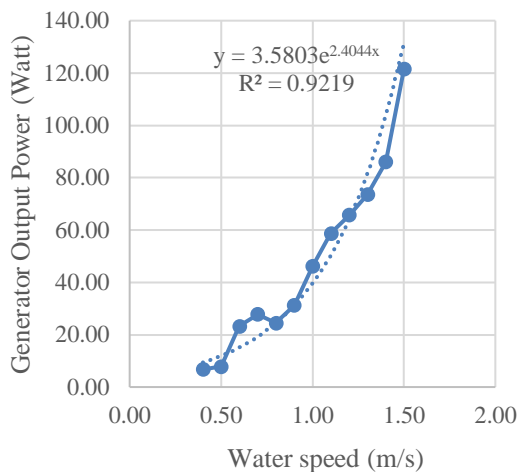


Figure 12. Correlation of electric power to the speed of water from the rotation of the wheel at an angle of 0°

The graph of the correlation between the generator rotation in rpm and water speed for the bending angle 0° on the pinwheels can be seen in Figure 13.

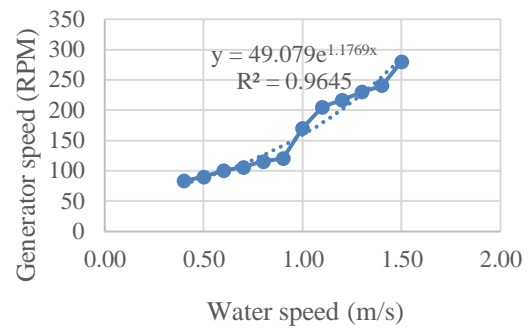


Figure 13. Correlation of the generator rotation to the speed of water for the grasshopper angle 0°

Figures 12 and 13 show there is no change in the length of the radius to the center of the wheel. The blade of the waterwheel moves to close and open when entering and leaving the water. Electrical power and the rotation of the generator (RPM) are more dominant due to the shape of the blades. The graph of the experimental results using the line theoretical equation approach provides an overview of the rate of change increase in power and generator rotation of 114.75 watts and 197.22 RPM over a water velocity range of 0.4 m/s to 1.5 m/s. The graph shows a pattern of exponential function characteristics with an upward trend, with changes in a ripple of electrical power and the rotation of the generator (RPM) which is not large because it is only influenced by the wheel blades that close and open when entering and leaving the water at an angle of 90°.

The graph of the correlation between the generator electric power and water speed for the bending angle of 30° on the pinwheels can be seen in Figure 14.

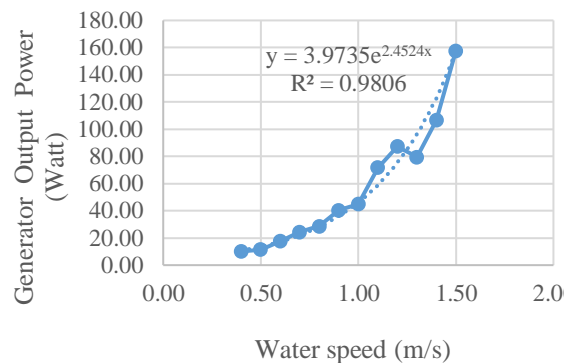


Figure 14. Electric power to water velocity for grasshopper angle 30°

The graph of the correlation between the generator rotation (rpm) and water speed for the bending angle of 30° on the pinwheels can be seen in Figure 15.

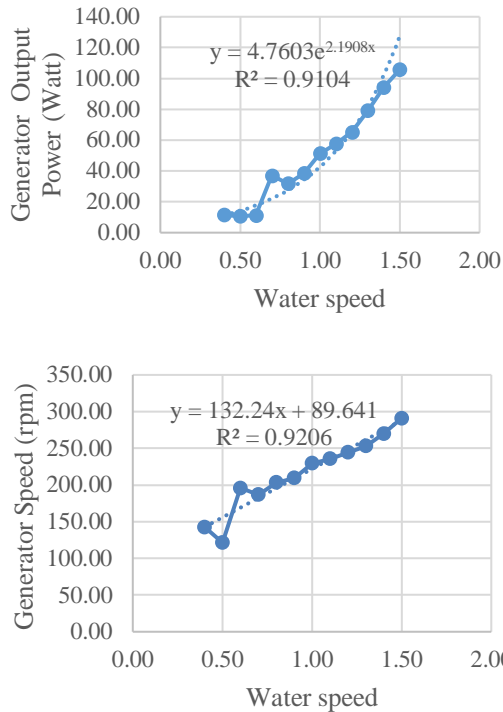


Figure 15. Rotation of the generator to the speed of water for the grasshopper angle of 30°

Figures 14 and 15 show the bending angle of 30° , where there is a change in the length of the radius to the center point of the wheel. The radius of the wheel that is bend makes the distance between the tip of the radius and the blade has a shorter distance than when it is straight, also the blade on the wheel closes and opens simultaneously with the change in the length of the radius when moving in and out of the water is more flexible. The characteristics of electrical power and the rotation of the generator (RPM) are caused by the shape of the butterfly blade and the bending angle of the radius of the wheel which makes it flexible to move. and the results of the images and graphs of the experimental results as well as the theoretical line equation approach provide an overview of the rate of change increase in power and generator rotation of 147.59 watts and 199.35 RPM in the water velocity range of 0.4 m/s to 1.5 m/s. The results of the electrical power

graph show the characteristic pattern of the exponential function and generator rotation (RPM) with a linear pattern with an upward trend, with changes ripple in electrical power and generator rotation that are not large because they are not only influenced by the wheel blades that close and open when entering and leaving the water, also influenced by changes in the length of the radius to the center point of the wheel which causes of pounding.

The graph of the correlation between the generator electric power and water speed for the bending angle of 45° on the pinwheels can be seen in Figure 16.

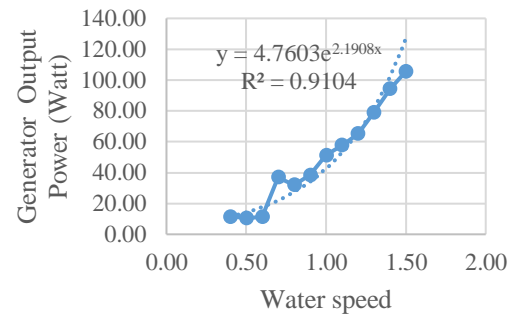


Figure 16. Electric power to the speed of the water at a grasshopper right angle 45°

The graph of the correlation between the generator rotation (rpm) and water speed for the bending angle of 45° on the pinwheels can be seen in Figure 17.

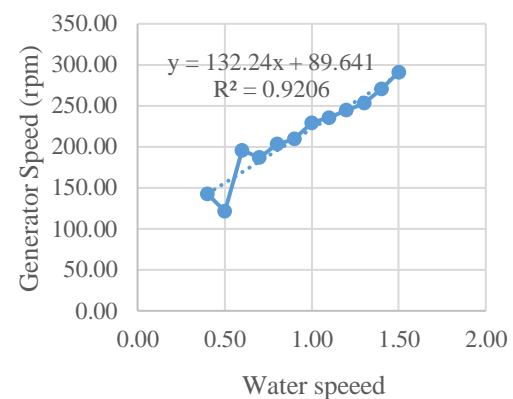


Figure 17. Rotation of the generator to the speed of the water at a grasshopper angle of 45°

Figures 16 and 17 show the 45° bending angle. There was an increase in power and generator rotation of 94.28 watts and 148.58 RPM at the water speed range of 0.4 m/s to

1.5 m/s. The electrical power graph showed a rippling change of electric power and generator rotation that it's getting bigger. It is influenced by the wheel blades closing and opening when entering and leaving the water, also influenced by changes in the length of the spokes to the center of the wheel.

The graph of the correlation between the generator electric power and water speed for the bending angle of 60° on the pinwheels can be seen in Figure 18.

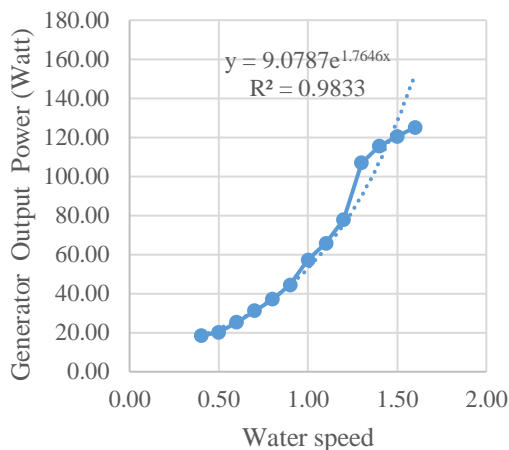


Figure 18. Electric power against the speed of the water at a grasshopper right angle 60°.

The graph of the correlation between the generator rotation (rpm) and water speed for the bending angle 60° on the pinwheels can be seen in Figure 19.

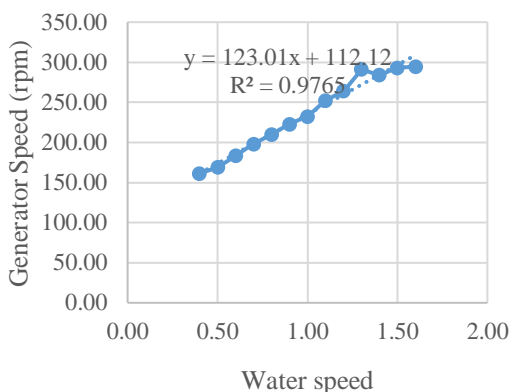


Figure 19. Rotation of the generator to the speed of the water at grasshopper angle 60°.

Figures 18 and 19 show the 60° bending angle. There was an increase in power and generator rotation are 102.12 watts and 132.03 RPM at the water velocity range of

0.4 m/s to 1.5 m/s. There is power instability and lower RPM rotation than other bending angles. There is a rippling change in the electric power and the generator rotation is getting bigger and more unstable.

The graph of the correlation between the generator electric power and water speed for the bending angle 90° on the pinwheels can be seen in Figure 20.

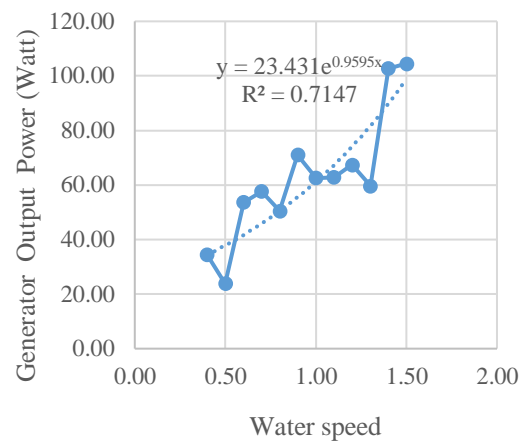


Figure 20. Electric power to the speed of the water at the grasshopper right angle 90°

The graph of the correlation between the generator rotation (rpm) and water speed for the bending angle of 90° on the pinwheels can be seen in Figure 21.

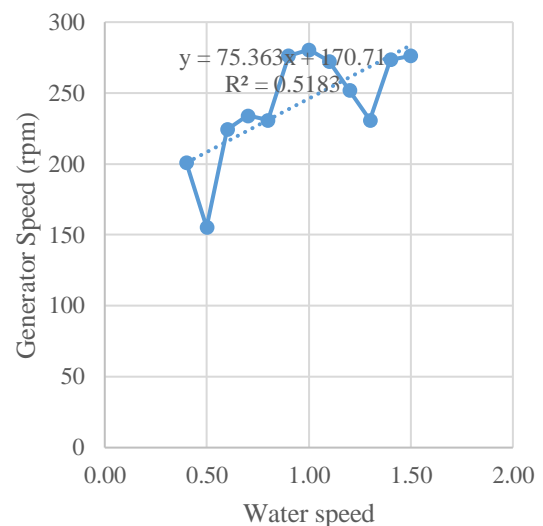


Figure 21. Rotation of the generator to the speed of the water at a grasshopper angle of 90°

Figures 20 and 21 show the 90° bending angle. The increase in power and generator

rotation shows 70.15 watts and 75.41 RPM at the water velocity range of 0.4 m/s to 1.5 m/s. The electrical power graph shows the same pattern as the previous bending angle, with changes in the electric power ripple and the generator rotation getting bigger and more unstable than bending angles 60° . At a bending angle of 90° , the effect of the gravitational force on the mass of the radius and the flexible blade is the widest from the previous angle, thus making the wheel spin slower because when it moves becomes heavier with the greatest pounding impact when it flips in the air before the blade enters the water.

The bending angle of the spokes of the grasshopper causes a change in the length of the spokes to the center of the wheel so that the spokes bend and make the distance between the tip of the spokes and the blade shorter when straight providing a stable impact on the wheel. The bending angle of 30° is the angle indicating the maximum effective performance of the wheel. This can be seen from the experimental values which tend to increase and are more stable than the bending angles of 0° , 45° , 60° , and 90° . At an angle of 30° , it provides a stable impact effect and strengthens wheel rotation without causing deceleration. When the angle is greater than 30 with a maximum at an angle of 90° , there will be a deceleration of the wheel rotation.

Figure 22 shows the shock when the wheel enters the surface of the water and when it comes out of the water because this flexibility causes the wheel to have a small resistance while in the water so that the rotation of the wheel is faster than the wheel with a constant blade and radius and not flexible. Figure 23 shows the shape of the flexible motion of the pinwheel while in the air. When the inflexible blades move out of the water, the water is carried upward by the blades, and the amount of water carried upward increases with increasing rotation speed. Water carried upward is considered a contributing factor to the reduction in turbine

efficiency (Adanta, 2018; Nishi et al., 2014; Siswantara et al., 2018)

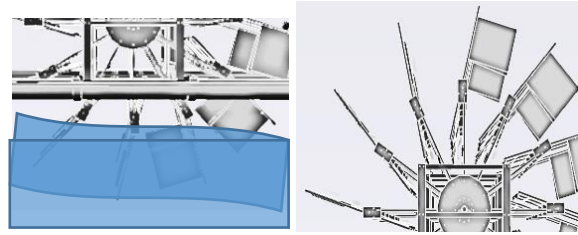


Figure 22. The pattern of water surfaces when the blade enters and leaves the water.

Figure 23. The shape of the flexible motion of the wheel in the air

The results of the development of the waterwheel model with the butterfly blade and grasshopper elbow spokes increase the flexibility of the blade and spokes, reducing the water carried upwards so that it can increase the rotating speed of the wheel when pushed by the airflow as has been done in the study on the undershot cross-flow air turbine with straight blades (Nishi et al., 2014; Nishi, et al., 2020; Yahagi et al., 2016).

The flexibility of the wheel occurs when entering and leaving the water surface and also when the wheel is in the air. The position of the radius of the pinwheel is from bending then moving in rotation until the position of the radius of the wheel is straight. The angle of the wheel perfectly opens simultaneously from an upright position at the very top position towards when it will enter the water surface.

The rpm rotation of the generator is generated from the speed of the water that drives the waterwheel and the generator which is loaded with a 200-watt lamp. The undershot waterwheel uses the flow from the waterwheel that hits or rotates the blade at the bottom of the wheel (Moe et al., 2019). The relationship of each change in bending angle of the grasshopper's radius produces different values during an increase in water speed It can be seen that the nature of the output has a change in electrical power and the generator rotation (RPM) fluctuates in

different intervals and an upward trend in the graph at an angle of 0° , 30° , 45° , 60° , and 90° .

This rapidly stretching and opening movement together gives a pounding effect. This is due to the influence of gravity on the mass of the radius and the flexible blade falling on the wheel so that it makes the wheel spin spontaneously fast at a certain angle. This has the opposite effect, resulting in slower rotation of the wheel as the bending angle of the trunk radius approaches the 90° angle. To eliminate the damage from the impact of the pounding effect on the supported radius, the part that is pounded is given a damper iron which works the same as a spring so that the part of the wheel that is pounded is not damaged. The magnitude of this pounding effect is influenced by the bending angle formed by the radius, so it affects the rotation of the generator and the electrical power it produces. At a bending angle of 30° , the influence of the gravitational force on the mass of the radius and the flexible blade is most effective that it makes the wheel spin faster, because when it moves with the most stable pounding and increases the thrust of the wheel rotation by the water when it flips in the air before the blade enters the water thus producing power electricity from a stable and optimum waterwheel.

CONCLUSION AND SUGGESTION

A Waterwheel with flexible pinwheels and blades produced a faster and more effective rotation than waterwheels with fixed pinwheels and blades. The Electrical energy at the angle of 30° of bending of the grasshopper's pinwheel with the butterfly blade was more optimal than at the angles of 0° , 45° , 60° , and 90° . Flexibility in the pinwheels and blades of the wheel provides less resistance when the wheel moves in the water so that the wheel can turn a pico hydro scale generator and generate electrical energy. The maximum efficiency of the wheel for the angle of 30° of buckling of the grasshopper's elbow radius is about 49.38% at a water speed of 1.5 m/s refers to table 3 Output power results (P_{out}) with total power

by the wheel at a speed of 1.5 m/s is 319.30 watts and table 4 conversion into electrical energy at a speed of 1.5 m/s is 157.66 watts. If the bending angle on the pinwheel is getting bigger, it will cause the waterwheel to spin slower. The efficiency of grasshopper pinwheels and butterfly blades is better than wheels with fixed pinwheels and blades. Suggestion for further research is to test waterwheels in rivers with weak and medium currents.

ACKNOWLEDGMENT

Thank you to the Institute for Research and Community Service, Palangkaraya State Islamic Institute for providing funding for this research

AUTHORS CONTRIBUTIONS

SH conducted a study of the design of the shape of the waterwheel that moves with the push of the water current and gives a pounding effect that increases the rotation of the waterwheel. RR and SA participated in making a waterwheel in the laboratory workshop room and conducting trials in the pool and retrieving experimental data. SF participates in compiling research designs, coordinating and helping to compile manuscripts, and data analysis. All authors read and approve the final manuscript.

REFERENCES

- Adanta, D., Kurnianto, M. A. F., Warjito, W., Nasution, S. B. S., & Budiarmo. (2020). Effect of the number of blades on undershot waterwheel performance for straight blades. *IOP Conference Series: Earth and Environmental Science*, 431(1). <https://doi.org/10.1088/1755-1315/431/1/012024>
- Adanta, D., Budiarmo, Warjito, & Siswantara, A. I. (2018). Assessment of turbulence modeling for numerical simulations into pico hydro turbine. *Journal of Advanced Research in Fluid Mechanics and Thermal Sciences*, 46(1), 21–31.
- Adanta, D., Budiarmo, Warjito, Siswantara, A. I., & Prakoso, A. P. (2018).

- Performance comparison of NACA 6509 and 6712 on pico hydro type cross-flow turbine by numerical method. *Journal of Advanced Research in Fluid Mechanics and Thermal Sciences*, 45(1), 116–127.
- Ali, B., & Kumar, A. (2017). Development of water demand coefficients for power generation from renewable energy technologies. *Energy Conversion and Management*, 143, 470–481. <https://doi.org/10.1016/j.enconman.2017.04.028>
- Arias-Gaviria, J., van der Zwaan, B., Kober, T., & Arango-Aramburo, S. (2017). The prospects for Small Hydropower in Colombia. *Renewable Energy*, 107, 204–214. <https://doi.org/10.1016/j.renene.2017.01.054>
- Balkhair, K. S., & Rahman, K. U. (2017). Sustainable and economical small-scale and low-head hydropower generation: A promising alternative potential solution for energy generation at local and regional scale. *Applied Energy*, 188, 378–391. <https://doi.org/10.1016/j.apenergy.2016.12.012>
- Brykała, D., & Podgórski, Z. (2020). Evolution of landscapes influenced by watermills, based on examples from Northern Poland. *Landscape and Urban Planning*, 198(October 2019), 87–100. <https://doi.org/10.1016/j.landurbplan.2020.103798>
- Denny, M. (2004). The efficiency of overshoot and undershot waterwheels. *European Journal of Physics*, 25(2), 193–202. <https://doi.org/10.1088/0143-0807/25/2/006>
- Dewatama, Fauziah, M., Safitri, H., & Adhisuwignjo, S. (2020). *Design and implementation: Portable Floating Design and implementation: Portable Floating Pico-Hydro*. <https://doi.org/10.1088/1757-899X/732/1/012049>
- Fajri, M. A., Elektro, T., & Sriwijaya, U. (2019). Desain Pembangkit Listrik Tenaga Piko hidro Menggunakan Program Arduino Uno Pada Penambahan Variasi Aliran Air . 23–24.
- Faria, F. A. M. d., & Jaramillo, P. (2017). The future of power generation in Brazil: An analysis of alternatives to Amazonian hydropower development. *Energy for Sustainable Development*, 41, 24–35. <https://doi.org/10.1016/j.esd.2017.08.001>
- Franco, W., Ferraresi, C., & Revelli, R. (2019). Functional analysis of piedmont (Italy) ancient water mills aimed at their recovery or reconversion. *Machines*, 7(2). <https://doi.org/10.3390/machines7020032>
- Ho-Yan, B. (2012). Design of a Low Head Pico Hydro Turbine for Rural Electrification in Cameroon. 1–175. <https://atrium.lib.uoguelph.ca/xmlui/handle/10214/3552>
- Irwan, L. K. W., Atus, B., Josefine, E. L., & Herby, C. P. T. (2019). Performance of undershot waterwheel curved blade of the laboratory scale. *Materials Science Forum*, 967 MSF, 250–255. <https://doi.org/10.4028/www.scientific.net/MSF.967.250>
- Jamlay, K., Sule, L., & Hasan, D. (2016). Analisis Perilaku Aliran Terhadap Kinerja Roda Air Arus Bawah Untuk Pembangkit Listrik Skala Piko hidro. *Dinamika Teknik Mesin*, 6(1). <https://doi.org/10.29303/d.v6i1.25>
- Junaidi, A., & Hendri, A. (2014). Model Fisik Kincir Air Sebagai Pembangkit Listrik. 1(2).
- Kholiq, I. (2015). Pemanfaatan Energi Alternatif sebagai Energi Terbarukan untuk Mendukung Substitusi BBM. In *Jurnal IPTEK* (Vol. 19, Issue No 2).
- Kougias, I., Aggidis, G., Avellan, F., Deniz, S., Lundin, U., Moro, A., Muntean, S., Novara, D., Pérez-Díaz, J. I., Quaranta, E., Schild, P., & Theodossiou, N. (2019). Analysis of emerging technologies in the hydropower sector. *Renewable and Sustainable Energy Reviews*, 113(June), 109257. <https://doi.org/10.1016/j.rser.2019.109>

- 257
- Krajačić, G., Vujanović, M., Duić, N., Kılıkış, Ş., Rosen, M. A., & Ahmad Al-Nimr, M. (2018). Integrated approach for sustainable development of energy, water, and environment systems. *Energy Conversion and Management*, 159 (3), 398–412. <https://doi.org/10.1016/j.enconman.2017.12.016>
- Lindawati, Jumarang, M. I., & Kushadiwijayanto, A. A. (2018). Karakteristik perambatan gelombang pasang surut di Estuari Kapuas Kecil. *Jurnal Laut Katulistiwa*, 1(3), 61–66. <https://jurnal.untan.ac.id/index.php/lk/article/view/29859>
- Manzano-Agugliaro, F., Taher, M., Zapata-Sierra, A., Juaidi, A., & Montoya, F. G. (2017). An overview of research and energy evolution for small hydropower in Europe. *Renewable and Sustainable Energy Reviews*, 75(May 2015), 476–489. <https://doi.org/10.1016/j.rser.2016.11.013>
- Masud, I. A., & Suwa, Y. (2018). Effect of Blade Inclination Angle on the Efficiency of Hydrokinetic Turbine in an Undershot Zero Head System. 6(6). <https://doi.org/10.18178/ijmmm.2018.6.6.413>
- McManamay, R. A., Parish, E. S., DeRolph, C. R., Witt, A. M., Graf, W. L., & Burner, A. (2020). Evidence-based indicator approach to guide preliminary environmental impact assessments of hydropower development. *Journal of Environmental Management*, 265(March), 110489. <https://doi.org/10.1016/j.jenvman.2020.110489>
- Ming, B., Liu, P., Cheng, L., Zhou, Y., & Wang, X. (2018). Optimal daily generation scheduling of large hydro-photovoltaic hybrid power plants. *Energy Conversion and Management*, 171(April), 528–540. <https://doi.org/10.1016/j.enconman.2018.06.001>
- Moe, K. P., Myat, E. E., Khaing, C. C., & NWE, Z. M. (2019). Design of 10 kW Water Wheel for Micro-Hydro Power. *International Journal of Scientific Engineering and Technology Research*, 08, 344–349.
- Moshfegh, B. (2011). World Renewable Energy Congress – Sweden Editor. *World Renewable Energy Congress - Sweden*, undefined-undefined.
- Müller, G., & Kauppert, K. (2004). Performance characteristics of water wheels. *Journal of Hydraulic Research*, 42(5), 451–460. <https://doi.org/10.1080/00221686.2004.9641215>
- Nishi, Y., Hatano, K., & Inagaki, T. (2017). Study on performance and flow field of an undershot cross-flow water turbine comprising different number of blades. *Journal of Thermal Science*, 26(5), 413–420. <https://doi.org/10.1007/s11630-017-0956-1>
- Nishi, Y., Hatano, K., Okazaki, T., Yahagi, Y., & Inagaki, T. (2020). Improvement of performance of undershot cross-flow water turbines based on shock loss reduction. *International Journal of Fluid Machinery and Systems*, 13(1), 30–41. <https://doi.org/10.5293/IJFMS.2019.13.1.030>
- Nishi, Y., Inagaki, T., Li, Y., & Hatano, K. (2015). Study on an Undershot Cross-Flow Water Turbine with Straight Blades. *International Journal of Rotating Machinery*, 2015. <https://doi.org/10.1155/2015/817926>
- Nishi, Y., Inagaki, T., Li, Y., Omiya, R., & Fukutomi, J. (2014). Study on an undershot cross-flow water turbine. *Journal of Thermal Science*, 23(3), 239–245. <https://doi.org/10.1007/s11630-014-0701-y>
- Nishi, Y., Yahagi, Y., Okazaki, T., & Inagaki, T. (2020). Effect of flow rate on performance and flow field of an undershot cross-flow water turbine. *Renewable Energy*, 149, 409–423. <https://doi.org/10.1016/j.renene.2019.12.023>

- Norhadi, A., Marzuki, A., Wicaksono, L., & Yacob, R. A. (2015). Studi Debit Aliran Pada Sungai Antasan Kelurahan Sungai Andai Banjarmasin Utara. *Jurnal Poros Teknik*, 7(1).
- Pérez-Sánchez, M., Sánchez-Romero, F. J., Ramos, H. M., & López-Jiménez, P. A. (2017). Energy recovery in existing water networks: Towards greater sustainability. *Water (Switzerland)*, 9(2), 1–20. <https://doi.org/10.3390/w9020097>
- Permanasari, A. A., Sukarni, Puspitasari, P., Utama, S. B., & Yaqin, F. A. (2019). Experimental Investigation and Optimization of Floating Blade Water Wheel Turbine Performance Using Taguchi Method and Analysis of Variance (ANOVA). *IOP Conference Series: Materials Science and Engineering*, 515(1). <https://doi.org/10.1088/1757-899X/515/1/012086>
- Pranoto, B., Aini, S. N., Soekarno, H., Zukhrufiyati, A., Rasyid, H. Al, & Lestari, S. (2018). (Studi Kasus Di Wilayah Sungai Serayu Opak) The Potential Of Microhydro In Irrigation Area (Case Study In Serayu Opak River Basin). 77–86.
- Punys, P., Kasiulis, E., Kvaraciejus, A., Dumbrasukas, A., Vyčienė, G., & Šilinis, L. (2017). Impacts of the EU and national environmental legislation on tapping hydropower resources in Lithuania – A lowland country. *Renewable and Sustainable Energy Reviews*, 80(March), 495–504. <https://doi.org/10.1016/j.rser.2017.05.196>
- Punys, P., Kvaraciejus, A., Dumbrasukas, A., Šilinis, L., & Popa, B. (2019). An assessment of micro-hydropower potential at historic watermill, weir, and non-powered dam sites in selected EU countries. *Renewable Energy*, 133, 1108–1123. <https://doi.org/10.1016/j.renene.2018.10.086>
- Quaranta, E., Katopodis, C., Revelli, R., & Comoglio, C. (2017). Turbulent flow field comparison and related suitability for fish passage of a standard and a simplified low-gradient vertical slot fishway. *River Research and Applications*, 33(8), 1295–1305. <https://doi.org/10.1002/rra.3193>
- Quaranta, E. (2018). Stream water wheels as renewable energy supply in flowing water: Theoretical considerations, performance assessment and design recommendations. *Energy for Sustainable Development*, 45, 96–109. <https://doi.org/10.1016/j.esd.2018.05.002>
- Quaranta, E. (2020). Estimation of the permanent weight load of water wheels for civil engineering and hydropower applications and dataset collection. *Sustainable Energy Technologies and Assessments*, 40(June), 100776. <https://doi.org/10.1016/j.seta.2020.100776>
- Quaranta, E., Bonjean, M., Cuvato, D., Nicolet, C., Dreyer, M., Gaspoz, A., Rey-Mermet, S., Boulicaut, B., Pratalata, L., Pinelli, M., Tomaselli, G., Pinamonti, P., Pichler, R., Turin, P., Turrin, D., Foust, J., Trumbo, B., Ahmann, M., Modersitzki, M., ... Bragato, N. (2020). Hydropower case study collection: Innovative low head and ecologically improved turbines, hydropower in existing infrastructures, hydropeaking reduction, digitalization and governing systems. *Sustainability (Switzerland)*, 12(21), 1–79. <https://doi.org/10.3390/su12218873>
- Quaranta, E., & Müller, G. (2018). Sagebien and Zuppinger water wheels for very low head hydropower applications. *Journal of Hydraulic Research*, 56(4), 526–536. <https://doi.org/10.1080/00221686.2017.1397556>
- Quaranta, E., & Revelli, R. (2017a). CFD simulations to optimize the blade design of water wheels. *Drinking Water Engineering and Science*, 10(1), 27–32. <https://doi.org/10.5194/dwes-10-27-2017>

- Quaranta, E., & Revelli, R. (2017b). Hydraulic Behavior and Performance of Breastshot Water Wheels for Different Numbers of Blades. *Journal of Hydraulic Engineering*, 143(1), 04016072. [https://doi.org/10.1061/\(asce\)hy.1943-7900.0001229](https://doi.org/10.1061/(asce)hy.1943-7900.0001229)
- Quaranta, E., & Revelli, R. (2018). Gravity water wheels as a micro hydropower energy source: A review based on historic data, design methods, efficiencies and modern optimizations. *Renewable and Sustainable Energy Reviews*, 97(November 2017), 414–427. <https://doi.org/10.1016/j.rser.2018.08.033>
- Quaranta, E., & Wolter, C. (2021). Sustainability assessment of hydropower water wheels with downstream migrating fish and blade strike modelling. *Sustainable Energy Technologies and Assessments*, 43(November 2020), 100943. <https://doi.org/10.1016/j.seta.2020.100943>
- Setyawan, E. Y., Djiwo, S., Praswanto, D. H., Suwandono, P., Siagian, P., & Malang, U. W. (2019). *Design of Low Flow Undershot Type Water Turbine*. 2(October), 50–55.
- Siswantara, A. I., Budiarmo, Prakoso, A. P., Gunadi, G. G. R., Warjito, & Adanta, D. (2018). Assessment of turbulence model for cross-flow pico hydro turbine numerical simulation. *CFD Letters*, 10(2), 38–48.
- Sritram, P., & Suntivarakorn, R. (2017). Comparative Study of Small Hydropower Turbine Efficiency at Low Head Water. *Energy Procedia*, 138, 646–650. <https://doi.org/10.1016/j.egypro.2017.10.181>
- Suhartono, Fatmawati, S., & Rudianto, R. (2017). Engineering of Floating Power Plant for River Flow Type Undershot 2 Waterwheels With 9 Fixed Blade and Butterfly Blade on Picohydro Scale. 8(1), 45–52.
- Sule, L., Mochtar, A. A., & Sutresman, O. (2020). Performance of undershot water wheel with bowl-shaped blades model. *International Journal of Technology*, 11(2), 278–287. <https://doi.org/10.14716/ijtech.v11i2.2465>
- Suparman. (2017). Desain Pembangkit Listrik Tenaga Piko Hidro. *Eeccis*, 11(2), 82–88.
- Warjito, Adanta, D., Budiarmo, & Prakoso, A. P. (2018a). The effect of bucket number on breastshot waterwheel performance. *IOP Conference Series: Earth and Environmental Science*, 105(1). <https://doi.org/10.1088/1755-1315/105/1/012031>
- Yah, N. F., Idris, M. S., & Oumer, A. N. (2016). Numerical Investigation on Effect of Immersed Blade Depth on the Performance of Undershot Water Turbines. *MATEC Web of Conferences*, 74, 5–9. <https://doi.org/10.1051/mateconf/20167400035>
- Yahagi, Y., Nishi, Y., Okagaki, T., & Inagaki, T. (2016). Performance analysis of an undershot cross-flow water turbine based on the flow near the runner. *Transactions of the JSME (in Japanese)*, 82(841), 16-00271-16-00271. <https://doi.org/10.1299/transjsme.16-00271>
- Zhou, Y., Chang, L. C., Uen, T. S., Guo, S., Xu, C. Y., & Chang, F. J. (2019). Prospect for small-hydropower installation settled upon optimal water allocation: An action to stimulate synergies of water-food-energy nexus. *Applied Energy*, 238(October 2018), 668–682. <https://doi.org/10.1016/j.apenergy.2019.01.069>